Arch. Min. Sci. **67** (2022), 4, 565-601

Electronic version (in color) of this paper is available: http://mining.archives.pl

DOI: https://doi.org/10.24425/ams.2022.143676

WOJCIECH ŻYGAS[1], JACEK BLICHARSKI[1*], CZESŁAW RYBICKI[1]

A COMPUTER AIDED ANALYSIS AND FORECASTING OF GAS RESERVOIR PRODUCTION

The article presents a methodology for analysing historical gas production data and determining the gas reserves and the petrophysical parameters of a reservoir-aquifer system. These parameters are obtained from a fitting algorithm using production data sets. A forecast of the future field gas production can be created on the calibrated mathematical model basis. The developed method is based on the material balance assumptions and the widely used Fetkovich and van Everdingen-Hurst equations for calculating water influx. To conduct the calculations and analyse production data, the computer application was developed using Python programming language. A user-friendly graphical interface makes the proposed application convenient and intuitive to use. The software was calibrated based on the literature data from the gas field of known parameters and then validated using five case studies of the actual gas fields in the Polish Carpathian Foredeep. From the tests, very high compatibility between the computed and the real field values were obtained. An additional comparison with the commercial program MatBal confirmed the proper functioning of the application.

Keywords: Computer application; Optimization; Gas production; Production forecasting; Energy conditions; Numerical analysis

Nomenclature

GUI – graphical user interface
GWC – gas-water contact
OGIP – original gas in place
UGS – underground gas storage
vEH – van Everdingen-Hurst

[1] AGH UNIVERSITY OF SCIENCE AND TECHNOLOGY, FACULTY OF DRILLING, OIL AND GAS, AL. MICKIEWICZA 30, 30-059 KRAKOW, POLAND

* Corresponding author: jblich@agh.edu.pl

B_{gi} – gas formation volume factor at initial reservoir pressure
B_{wj} – water formation volume factor calculated for the p_j pressure
C_f – formation compressibility (1/Pa)
C_w – water compressibility (1/Pa)
E_g – gas expansion factor
F – cumulative amount of the produced fluids at reservoir conditions (m^3)
f – fractional encroachment angle
G_i – gas initially in place (Nm^3)
G_{Ij} – cumulative gas injected for the time step j (Nm^3)
G_{pj} – cumulative gas production for the time step j (Nm^3)
G_p – cumulative gas production (Nm^3)
h – formation thickness (m)
J – aquifer productivity index ($m^3/(Pa \cdot s)$)
k – permeability of a reservoir-aquifer system (mD, 1 mD ≈ 10^{-15} m^2)
$p_{a\,(j-1)}$ – average pressure in an aquifer during the time step previous to the time step j (Pa)
p_i – initial pressure in a reservoir-aquifer system (Pa)
p_j – reservoir pressure for the time step j (Pa)
p_{rj} – average reservoir-aquifer boundary pressure during the time step j (Pa)
r_a – aquifer radius (m)
r_e – reservoir radius (m)
t_j – the time from the beginning of the production for the time step j (s)
U – aquifer constant (m^3/Pa)
W_D – dimensionless water influx calculated as a function of the dimensionless radius r_D and the dimensionless time t_D
W_{ei} – maximum possible water influx (m^3)
W_{ej} – cumulative water influx calculated for the p_j pressure (m^3)
W_i – the initial volume of water in the aquifer (m^3)
W_{pj} – cumulative water produced for the time step j (m^3)
Z_i – compressibility factor at initial reservoir pressure
Z_j – compressibility factor calculated for the p_j pressure
ΔW_{ex} – the water influx during the time step x (m^3)
μ_w – water dynamic viscosity ($Pa \cdot s$)
ϕ – porosity

1. Introduction

Forecasting the production of oil and gas fields responds to the complex contemporary challenges of today's petroleum industry. Determining the cost-effectiveness of the production process is one example. Combining in-depth specialised knowledge with computer science is the foundation of ubiquitous automation and informatisation. Computers, machines and sensors form an industrial control system, which presents selected information to the end user. Industrial transformation modifies the role of the modern engineer, whose main duty is to analyse data displayed on a computer screen.

The need to analyse and manage a large number of data results in the implementation of new software solutions based on complex calculation algorithms. Effective production management makes it possible to increase the recovery factor in the shortest possible time, using the primary reservoir energy efficiently. In gas fields, the main source of lifting energy is the energy of expanding gas. If the gas reservoir is in communication with a surrounding active aquifer, water influx may be an additional source of energy, which supports the reservoir pressure. However, water influx is connected with moving the GWC (gas-water contact), which entails a risk of coning water towards production wells. The formation may develop so-called “water tongues” or “water cones” [1-3]. The frequency of occurrence of such adverse phenomena is affected by the method of reservoir exploitation, the production rate and, above all, the anisotropy of the reservoir rock.

Because natural gas extraction is a highly complex process, there is a need to develop calculation algorithms which use more or less advanced mathematical models. The aim is to properly evaluate reservoir parameters and credibly forecast further production [4,5]. Reservoir-drive mechanisms have to be considered as a fundamental part of the algorithms, including not only the primary gas drive mechanism but also some more complex ones connected with the changes in pore volume resulting from the influx of water into the reservoir [6,7]. The use of advanced IT solutions allows for the effective implementation of numerical calculation methods, which generates powerful simulation outcomes. The main limitation of concurrent commercial reservoir simulators is the time required to build a numerical model of the reservoir and its validation.

Using Python programming language along with its open-source scientific libraries (SciPy, scikit-learn, NumPy) and its bindings for widget toolkit (PyQt5, PyQtChart), a proprietary computer application was developed and controlled via a clear GUI (graphical user interface). The application supports the process of forecasting the exploitation of a gas field based on historical and current well production data as well as the parameters describing a gas reservoir and an aquifer. The functionality includes parameters for analyzing energy conditions in which the field operates. The application allows the user to make a long-term forecast concerning the possibility of gas injection into the reservoir, which extends the scope of applicability of a UGS (underground gas storage).

2. Methodology

2.1. The assumptions of the mathematical model

Assumptions and limitations were introduced to describe the processes taking place in the reservoir. The extracted gas was zero or low condensate-content gas (dry gas). It was defined as a mixture of components whose contents were provided by the user. These components include methane, ethane, propane, isobutane, n-butane, carbon dioxide, nitrogen, hydrogen sulfide and helium. The anisotropy of the reservoir rocks was not considered. Consequently, the petrophysical parameters describing a gas reservoir and an aquifer have constant values regardless of the direction. The mathematical model includes the process of gas injections as well as the possibility of increasing the water cut. In the calculation algorithm, the process of the exploitation of a gas field was designed as a discrete-event simulation, in which the values of parameters were recalculated in each discrete time step, specified by the user.

2.2. The algorithm of calculations

The application allows the user to determine the parameters describing a gas reservoir and an aquifer based on historical well production data. These parameters are used to forecast further exploitation of the gas field concerning the possibility of gas injection into the reservoir. The mathematical model consists of material balance equations and natural water influx equations according to vEH (van Everdingen-Hurst) and Fetkovich methods [1,3,8]. These two methods of calculating water influx are well-documented in literature and widely used in the industry. During application development, the results of these methods were compared to each other to minimalise the probability of an error. Furthermore, supplementary formulas used to determine the PVT properties of the reservoir fluids were implemented. From the user's perspective, any additional functionality increases the likelihood of achieving a well-calibrated mathematical model.

During the exploitation of the water drive gas reservoir, the compressed water flows gradually from the aquifer into the reservoir, supporting the pressure within the pore spaces [9]. The volume and the intensity of water influx depend on the size of the aquifer, the activity of the water drive, the petrophysical parameters of the reservoir rocks, the PVT properties of the reservoir fluids, the production rate, and the OGIP (original gas in place). The values associated with these factors are determined by solving the dependent system of the material balance and the natural water influx equations, using the parameters describing the gas reservoir and the aquifer provided by the user [2,10,11]. The criterion of correctness constitutes compliance between the computed values of the reservoir pressure and its actual values. The solution to this issue requires the use of the optimisation method for the so-called inverse problem [12] (Fig. 1).

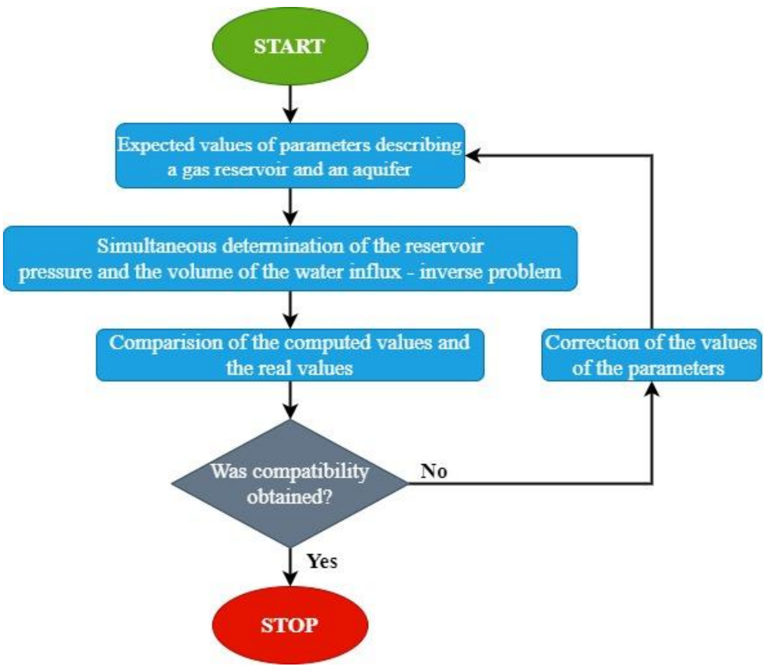

Fig. 1. The algorithm of calculations performed by the application

This results from the lack of knowledge about the actual values of the parameters describing the reservoir-aquifer system. The algorithm applied in the application operates depending only on the probable values entered by the user. It is based on the iteration equations allowing for simultaneous determination of the reservoir pressure and the volume of water influx. The actual values of pressure provide a reference for the values computed in each time step j. Consequently, the result of the comparison acts as positive feedback, used to correct the value of the determining parameter. The calculations, which use the successive approximation method, operate in the loop until very high compliance between the computed values and the actual values is obtained. This is the so-called model calibration.

2.3. The mathematical model of calculations

The form of the material balance equations, which includes water influx into the reservoir and the production of water, for the time step j can be described by the following equation [13,14]:

$$\left(\frac{p_j}{Z_j}\right) = \frac{p_i}{Z_i} \cdot \frac{\left(1 - \frac{G_{pj} - G_{Ij}}{G_i}\right)}{1 - \frac{W_{ej} - B_{wj} \cdot W_{pj}}{G_i \cdot B_{gi}}} \tag{1}$$

where:

- B_{gi} – gas formation volume factor at initial reservoir pressure,
- B_{wj} – water formation volume factor calculated for the p_j pressure,
- G_i – original gas in place (Nm^3),
- G_{Ij} – cumulative gas injected for the time step j (Nm^3),
- G_{pj} – cumulative gas production for the time step j (Nm^3),
- p_i – initial pressure in a reservoir-aquifer system (Pa),
- p_j – reservoir pressure for the time step j (Pa),
- W_{ej} – cumulative water influx calculated for the p_j pressure (m^3),
- W_{pj} – cumulative water produced for the time step j (m^3),
- Z_i – compressibility factor at initial reservoir pressure,
- Z_j – compressibility factor calculated for the p_j pressure.

Next, water influx into the reservoir is formed according to the chosen method. The Fetkovich method uses equations from 2 to 8 to describe water influx. While equations from 9 to 12 refer to the vEH method.

2.3.1. Fetkovich method

According to the Fetkovich method, the cumulative water influx into the reservoir can be described by the equation:

$$W_{ej} = \sum_{x=1}^{j} \Delta W_{ex} \tag{2}$$

where: ΔW_{ex} – the water influx during the time step x (m^3).
The remaining symbols are defined above.

The value of water influx during the time step j ΔW_{ej} can be calculated using the following formula [1,15]:

$$\Delta W_{ej} = \frac{W_{ei}}{p_i}\left(p_{a(j-1)} - p_{rj}\right) \cdot \left(1 - \exp\left(\frac{-J \cdot p_i \cdot \left(t_j - t_{(j-1)}\right)}{W_{ei}}\right)\right) \tag{3}$$

where:

- J – aquifer productivity index ($m^3/(Pa \cdot s)$),
- $p_{a\,(j-1)}$ – average pressure in an aquifer during the time step previous to the time step j (Pa),
- p_{rj} – average reservoir-aquifer boundary pressure during the time step j (Pa),
- t_j – time from the beginning of the production for the time step j (s),
- W_{ei} – maximum possible water influx (m^3).

The remaining symbols are defined above.

The productivity index can be described by:

$$J = \frac{2 \cdot \pi \cdot f \cdot k \cdot h}{\mu_w \cdot \left(\ln\ln\frac{r_a}{r_e} - 0,75\right)} \tag{4}$$

where:

- f – fractional encroachment angle,
- h – formation thickness (m),
- k – permeability of a reservoir-aquifer system (m^2),
- r_a – aquifer radius (m),
- r_e – reservoir radius (m),
- μ_w – water dynamic viscosity ($Pa \cdot s$).

The maximum possible water influx can be described by:

$$W_{ei} = \left(C_w + C_f\right) \cdot W_i \cdot p_i \cdot f \tag{5}$$

where:

- C_f – formation compressibility (1/Pa),
- C_w – water compressibility (1/Pa),
- W_i – initial volume of water in the aquifer (m^3),

The remaining symbols are defined above.

Next, the initial volume of water in the aquifer can be described by:

$$W_i = \pi \cdot \left(r_a^2 - r_e^2\right) \cdot h \cdot \phi \tag{6}$$

where: ϕ – porosity.

The remaining symbols are defined above.

The average pressure in an aquifer during the time step j can be described by:

$$p_{aj} = p_i \cdot \left(1 - \frac{\sum_{x=1}^{j} \Delta W_{ex}}{W_{ei}}\right) \tag{7}$$

in which the symbols are the same as the aforementioned.

The average reservoir-aquifer boundary pressure during the time step j can be described by:

$$p_{rj} = \frac{p_{(j-1)} + p_j}{2} \tag{8}$$

in which the symbols are the same as the aforementioned.

2.3.2. Van Everdingen-Hurst method

According to the vEH method, the cumulative water influx into the reservoir can be described by [16- 17]:

$$W_{ej} = U \cdot \frac{p_i - p_1}{2} \cdot W_D\left(t_D\left(t_1\right), r_D\right) + U \cdot \sum_{x=1}^{j-1}\left(\frac{p_{x-1} - p_{x+1}}{2} \cdot W_D\left(t_D\left(t_j - t_x\right), r_D\right)\right) \tag{9}$$

where:

U – aquifer constant (m^3/Pa),
W_D – dimensionless water influx calculated as a function of the dimensionless radius r_D and the dimensionless time r [1,13,14],
p_1 – average reservoir pressure after time t_1.

The remaining symbols are defined above.

The aquifer constant can be described by:

$$U = 2 \cdot \pi \cdot \phi \cdot \left(C_w + C_f\right) \cdot r_e^2 \cdot h \cdot f \tag{10}$$

in which the symbols are the same as the aforementioned.

The dimensionless radius can be described by:

$$r_D = \frac{r_a}{r_e} \tag{11}$$

in which the symbols are the same as the aforementioned.

The dimensionless time can be described by:

$$t_D = \frac{k \cdot t_j}{\phi \cdot \mu_w \cdot \left(C_f + C_w\right) \cdot r_e^2} \tag{12}$$

in which the symbols are the same as the aforementioned.

2.4. Determination of parameters' values

The application allows determining the values of ten parameters describing a gas reservoir and an aquifer: C_f, C_w, f, G_i, h, k, r_D, r_e, μ_w, and ϕ. However, to address this issue, some serious technical difficulties had to be overcome.

Firstly, solving the dependent system of the material balance and the natural water influx equations is very difficult due to the high number of imponderables. Consequently, there is also a considerable number of solutions which provide very high compatibility between the computed values and the real values [10]. Additionally, they are related to local extrema. It is unfavourable because optimisation algorithms search for the best-fitted value until they find a local minimum. As a consequence, calculations often get stuck on the first local minimum. This scenario is highly probable considering a large number of variables.

Secondly, another issue is achieving the values which are realisable for an actual reservoir. Notwithstanding very high compliance, the computed values might be overestimated or underestimated. It has a significant influence on the correctness of further forecasting.

The application uses the least_squares optimisation algorithm from the SciPy library to solve nonlinear problems [18]. The algorithm operates based on an iterative procedure. Similarly to different optimisation tools, this one finds a local minimum of the cost function [18]. Nevertheless, the problems related to getting stuck on the incorrect local minimum may be overcome by the proper setting of the least_squares parameters [18]. On account of that, a series of automation tests were done to define these parameters. The test results were saved in a spreadsheet and analysed afterwards.

First and foremost, the calculation method was chosen. The least_squares algorithm supports three algorithms to perform optimisation: the Trust Region Reflective method, the Levenberg-Marquardt algorithm and the dogleg algorithm [18]. The first one was selected because of the high accuracy, even when the starting points are far from the expected solution [19]. Furthermore, the Trust Region Reflective method allows solving problems with bounds on the values [18]. The completed automation tests verified that the chosen method is the most efficient.

Taking the features of the Trust Region Reflective method into account, the limits of the determining reservoir parameters were established based on literature data [20-23]. Broad ranges between limiting values were set. The possibility to narrow these ranges by the user was also allowed. Based on the above, both the high functionality and the accuracy of calculations were achieved.

The nonlinear optimisation, conducted using the application, has ten degrees of freedom. They are defined as independent values which affect the final results. The user can reduce the degrees of freedom to seven by using the additional features of the application. These functionalities were developed by implementing the McCain correlation for the water dynamic viscosity [23], the Newman correlations and the Hall correlation for the formation compressibility [21], and the p/Z material balance method to estimate the OGIP. Applying these features allows for reduced calculations and consequently improves the final results. It is crucial if the starting points are far from the expected solution. The described functionalities are non obligatory. The user can use them or stay with the standard optimisation method.

Moreover, the HO (Havlena-Odeh [24-26]) diagnostic plots were implemented. They can be used to assess the energy conditions of a reservoir (Cole plot) and verify the accuracy of the parameters describing an aquifer and the OGIP, which were obtained via optimisation [14,27].

3. Software functionality

3.1. Graphical User Interface

The proper presentation of the results is a crucial part of a user-friendly application. Thus, the application should be both intuitive and error-proof. Therefore, all problems must be predicted in advance – those caused by the lack of user attention and those connected with faulty data sets describing the reservoir-aquifer system. This was done based on a series of functional tests, which validated all of the user's needs.

The application can be split into the main application window (Fig. 2) and the results application window (Figs 3, 4). Additionally, the spreadsheet, which is used to export the obtained

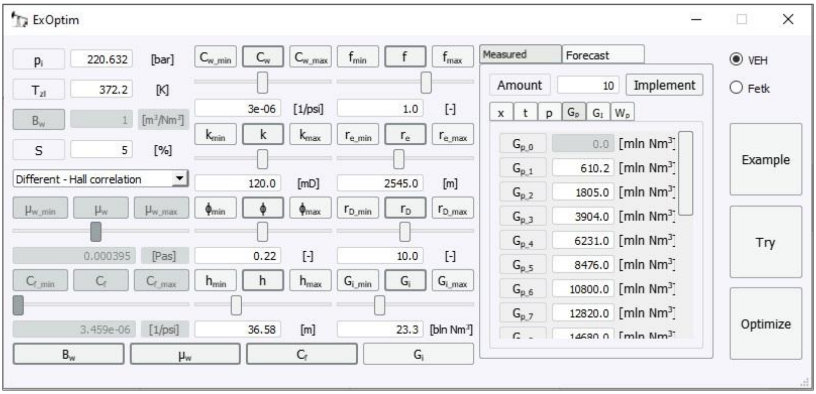

Fig. 2. The main application window

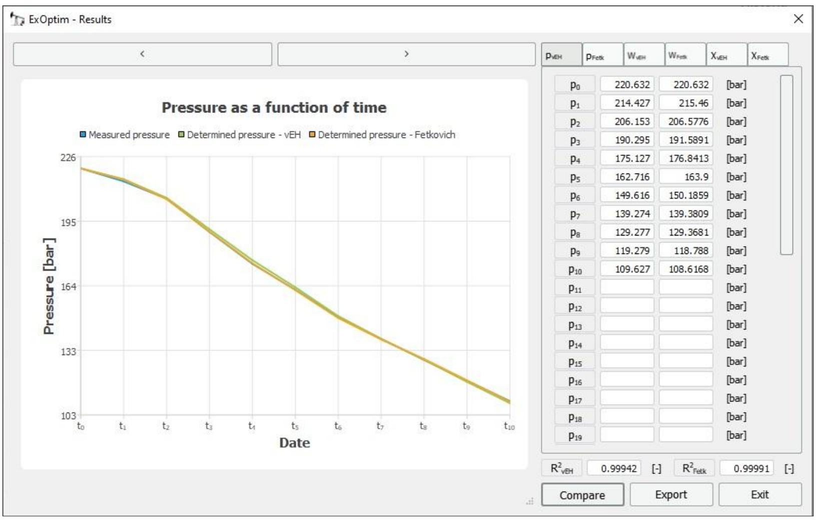

Fig. 3. The results application window – pressure as a function of time for the exemplary reservoir [13]

results, is also a valid part of communication with the user. The main application window is displayed directly after the application starts. In the beginning, text boxes are filled with sample data which can be replaced by the user by entering new values or importing the data of an actual gas reservoir. The results were illustrated graphically, and their interpretation was presented in the results application window. It is displayed after the completion of all calculations which were previously initiated.

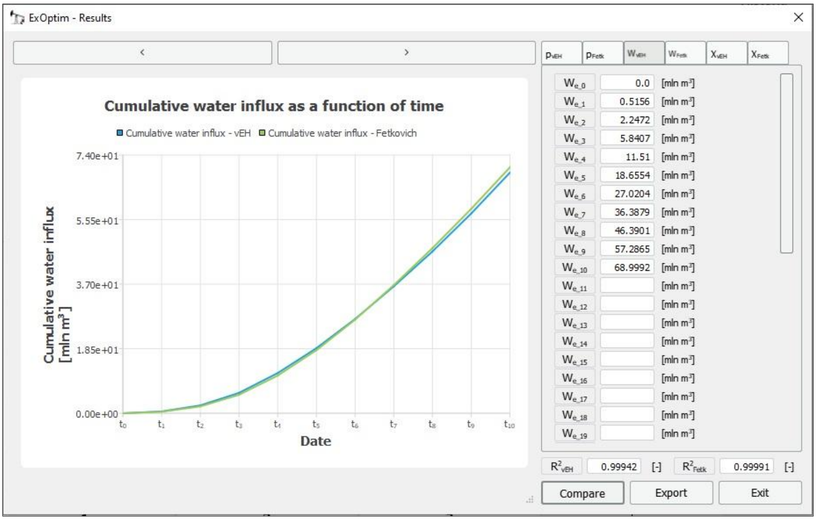

Fig. 4. The results application window – cumulative water influx as a function of time for the exemplary reservoir [13]

In the main application window, the data error control was implemented (Fig. 5). After finding an error, the text box is surrounded by a red frame. The calculations cannot continue until all errors are corrected.

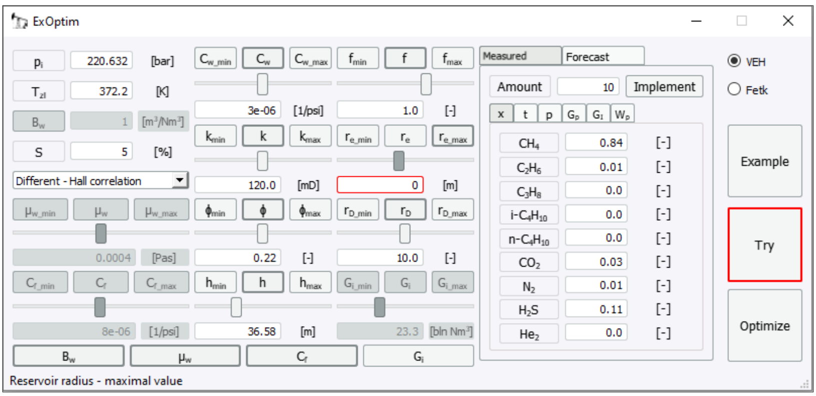

Fig. 5. The main application window – data error control

3.2. Application operation diagram

The way the application works from the user's perspective is presented in the diagram (Fig. 6). The first step is submitting input data either by inserting one's values or using the already provided

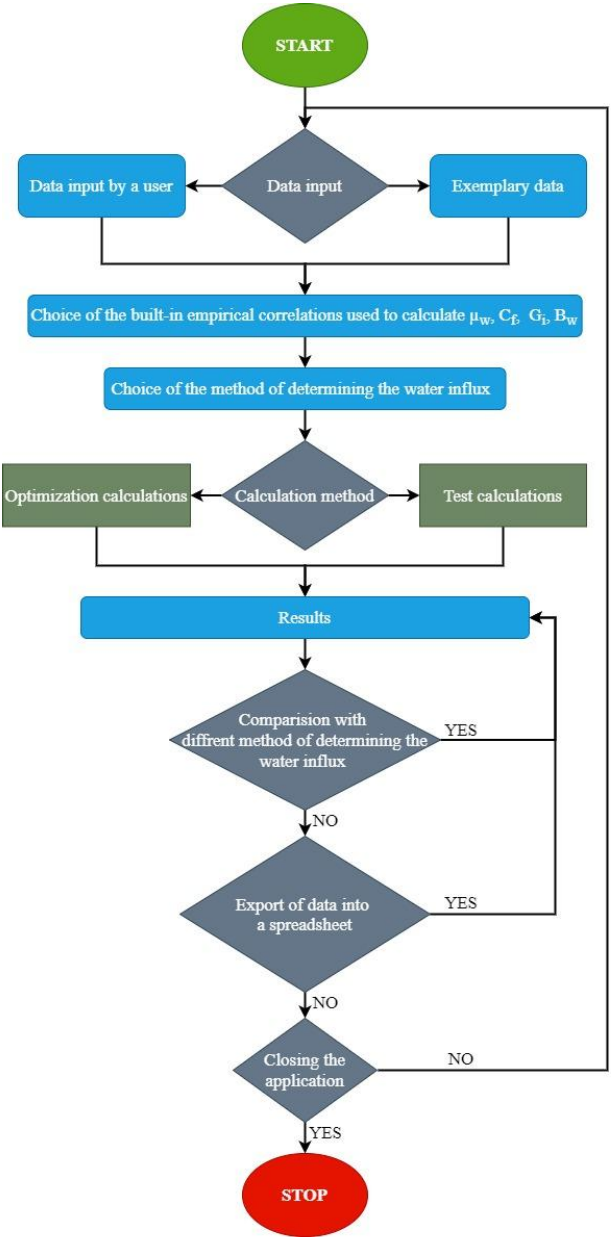

Fig. 6. Operating diagram from a User perspective

example. The main task of the application is optimising the input parameters, but it also allows for calculating several of them (the water formation volume factor, the water dynamic viscosity, the formation compressibility, and the OGIP) based on the built-in empirical correlations. The application also enables the user to verify the correctness of the provided values of parameters, disregarding the optimisation function (the mathematical model calculates based directly on the input data given by the user). After the calculations, the results of both methods of determining the influx of water into the reservoir are obtained. The generated values, as well as the diagrams, can be exported into a spreadsheet.

4. Results

In the initial phase of testing the program, the literature data from an exemplary reservoir was used [13]. The first software validation was performed based on that. The final evaluation of the application involved testing it while using the data from the high-methane gas reservoirs in the Carpathian Foredeep [28]. Five exemplary reservoirs, named A, B, C, D and E, were analysed using the application.

Based on geological data, geophysical profiles and the production process of the selected gas reservoirs, the estimated values and the limits of variables of the following parameters – the formation thickness, the porosity, the permeability of the reservoir-aquifer system, and the OGIP, were obtained. Additionally, the built-in empirical correlations were used to calculate the water dynamic viscosity, the formation compressibility, and the water formation volume factor. The remaining parameters and their limits were estimated while considering the typical values for the reservoirs in this part of the country.

The data necessary for carrying out the application analyses of the selected reservoirs was provided below, along with the analysis results. Input data contains the historical production data (Tables: A1, B1, C1, D1, E1), gas compositions data (Tables: A2, B2, C2, D2, E2), the estimated values of the parameters and their limits (Tables: 1, 3, 5, 7, 9). The output data includes determining values of the parameters (Tables: 2, 4, 6, 8, 10), statistical measures (Tables: A3, B3, C3, D3, E3) and plots describing a calibration model and its results. Plots of pressure as a function of time (Figs: 7, 9, 11, 13, 15) and cumulative water influx as a function of time (Figs: 8, 10, 12, 14, 16) are based directly on the obtained results. Whereas Coles plots (Figs: A1, B1, C1, D1, E1) and HO plots (Figs: A2, B2, C2, D2, E2) are used as diagnostic tools. Calculations of water influx for every reservoir were done using both vEH and Fetkovich methods.

Diagnostic plots allow for carrying out an in-depth analysis of reservoir exploitation, which might be used to decide on further production. The Cole plot shows the quotient of F (the cumulative amount of the produced fluids at reservoir conditions) and Eg (the gas expansion factor) in the function of Gp (the cumulative gas production). Points on Cole's plot reflect an aquifer activity. When the points are located horizontally, the reservoir is volumetric. The more the curve is inclined towards the top, the more active the aquifer is. During the exploitation of a reservoir with a moderate aquifer, the curve tends to fall after the initial increase. This is an indicator of the decrease in the activity of an aquifer. The HO plot shows the quotient of F and Eg in the function of the quotient of We and Eg. It allows for the evaluation of the mathematical model and the determined parameters. When the points on the plot are in line with the straight line with the slope equal to one, then the mathematical model was matched properly. Points inclined to the top or the bottom are indicators of incorrect calibration of the model. Too weak an aquifer reflects in top inclination, while too strong an aquifer in bottom inclination. The determination of the OGIP can be carried out by the extrapolation of the trend line to the y-axis.

4.1. Analysis of reservoir A

The example of reservoir A presents the evaluation of compatibility between the determined values and the production data. The data covered a twenty-three-year-long period of production (Table A1). The average reservoir temperature equalled 325 K.

TABLE 1

Estimated values and limits of the parameters – Reservoir A

Parameter	Input value	Min. value	Max. value
G_i [bln Nm^3]	5.10	5.00	5.20
C_w [1/Pa]	$5.80 \cdot 10^{-10}$	$2.90 \cdot 10^{-10}$	$8.70 \cdot 10^{-10}$
k [mD]	100	50	500
ϕ [–]	0.2	0.1	0.4
h [m]	75	50	200
f [–]	0.5	0.1	1
r_e [m]	2,000	500	10,000
r_D [–]	5	2	10

The determined parameters, excluding the fractional encroachment angle, have similar values for the two methods of calculating water influx (Table 2). The calculated pressures are almost equal to the measured pressures. The first difference can be noticed at the end of the production process (Fig. 7). The amount of the water influx is slightly larger for the Fetkovich method (Fig. 8). The coefficient of determination for the Fetkovich method is equal to 0.99904, while for the vEH method to 0.99900 (Table A3). The activity of the aquifer can be considered as low (Fig. A1). Despite some deviations between particular points in the plot F/E_g vs. We/E_g, they are in accordance with the straight line with the slope equal to one (Fig. A2). It indicates the proper selection of the values of the parameters.

TABLE 2

Determined values of the parameters – Reservoir A

Parameter	Output value	
	Fetkovich	van Everdingen Hurst
G_i [bln Nm^3]	5.200	5.200
C_w [1/Pa]	$4.84 \cdot 10^{-10}$	$5.13 \cdot 10^{-10}$
k [mD]	61.778	54.141
ϕ [–]	0.1789	0.1788
h [m]	66.598	50.412
f [–]	0.1913	0.2785
r_e [m]	1,614.03	1,808.88
r_D [–]	6.1103	5.0544

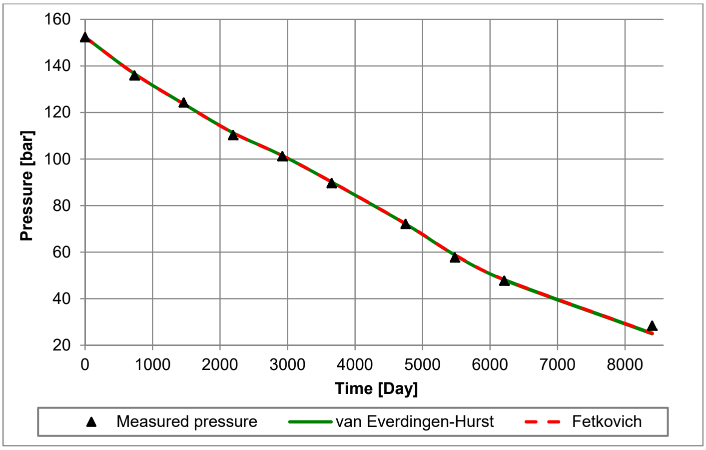

Fig. 7. Pressure as a function of time for the reservoir A

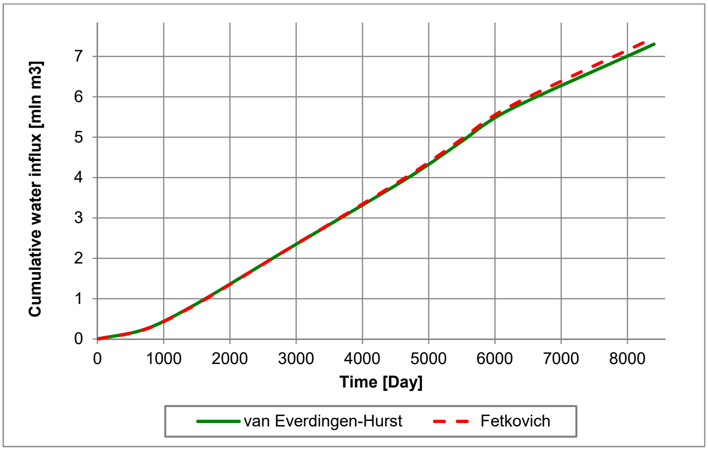

Fig. 8. Cumulative water influx as a function of time for the reservoir A

4.2. Analysis of reservoir B

The example of reservoir B presents the evaluation of compatibility between the determined values and the production data. The data covered a nine-year-long period of production (Table B1). The average reservoir temperature equalled 299 K.

The determined parameters, excluding the fractional encroachment angle and the dimensionless radius, have similar values for the two methods of calculating water influx (Table 4). The calculated pressures are nearly equal to the measured pressures during the production process (Fig. 9). The amount of the water influx is larger for the vEH method (Fig. 10). The coefficient of determination for the Fetkovich method is equal to 0.99887, while for the vEH method to 0.99886 (Table B3). The aquifer can be considered active (Figure B1). Despite some deviations between particular points in the plot F/Eg vs. We/Eg, they are in accordance with the straight

TABLE 3

Estimated values and limits of the parameters – Reservoir B

Parameter	Input value	Min. value	Max. value
G_i [bln Nm^3]	0.19	0.185	0.195
C_w [1/Pa]	$5.80 \cdot 10^{-10}$	$2.90 \cdot 10^{-10}$	$8.70 \cdot 10^{-10}$
k [mD]	250	100	500
ϕ [–]	0.2	0.1	0.3
h [m]	10	5	20
f [–]	0.5	0.1	1
r_e [m]	2,000	500	5,000
r_D [–]	5	2	10

line with the slope equal to one (Fig. B2). It indicates the proper selection of the determined values of the parameters.

TABLE 4

Determined values of the parameters – Reservoir B

Parameter	Output value	
	Fetkovich	van Everdingen Hurst
G_i [bln Nm^3]	0.195	0.192
C_w [1/Pa]	$6.71 \cdot 10^{-10}$	$6.12 \cdot 10^{-10}$
k [mD]	300.855	216.857
ϕ [–]	0.2118	0.2110
h [m]	9.119	8.829
f [–]	0.2670	0.4322
r_e [m]	2,154.76	2,317.94
r_D [–]	7.7857	6.1057

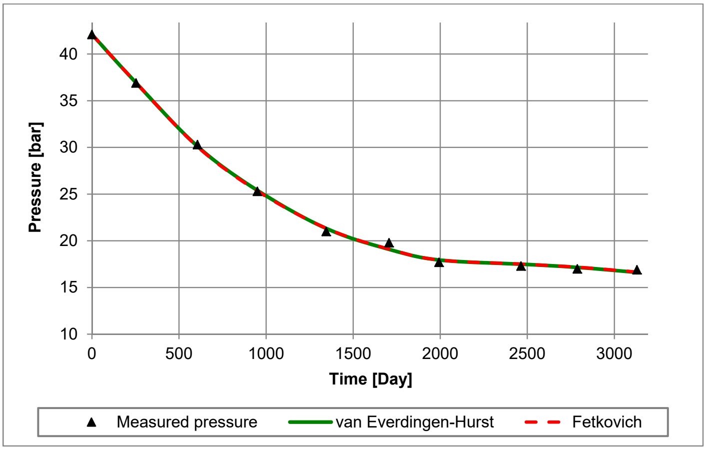

Fig. 9. Pressure as a function of time for the reservoir B

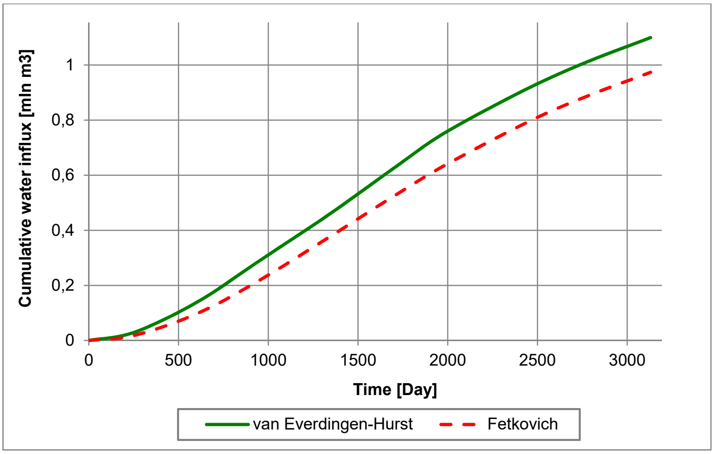

Fig. 10. Cumulative water influx as a function of time for reservoir B

4.3. Analysis of reservoir C

The example of reservoir C presents the evaluation of compatibility between the determined values and the production data. The data covered a thirteen-year-long period of production (Table C1), with the average reservoir temperature equal to 333 K. The gas contains mostly methane. However, the mole percentage of nitrogen is also significant (Table C2).

TABLE 5

Estimated values and limits of the parameters – Reservoir C

Parameter	Input value	Min. value	Max. value
G_i [bln Nm^3]	5.00	4.00	6.00
C_w [1/Pa]	$5.80 \cdot 10^{-10}$	$2.90 \cdot 10^{-10}$	$8.70 \cdot 10^{-10}$
k [mD]	30	10	60
ϕ [–]	0.15	0.1	0.2
h [m]	30	10	50
f [–]	0.5	0.1	1
r_e [m]	2,000	500	10,000
r_D [–]	10	2	20

The determined parameters, excluding the porosity, are slightly different for the two methods of calculating water influx (Table 6). Initially, the calculated pressures are equal to the measured pressures. While the trend is the same during the entire exploitation, minor differences are shown in the second half of the production period (Fig. 11). The amount of the water influx is slightly larger for the vEH method (Fig. 12). The coefficient of determination for the Fetkovich method is equal to 0.98839, while for the vEH method to 0.99259 (Table C3). The aquifer can be considered as active (Fig. C1). The points in the plot F/Eg vs. We/Eg are in accordance with the straight line with the slope equal to one (Fig. C2). It indicates the proper selection of the values of the parameters.

TABLE 6

Determined values of the parameters – Reservoir C

Parameter	Output value	
	Fetkovich	van Everdingen Hurst
G_i [bln Nm^3]	5.967	5.533
C_w [1/Pa]	$6.88 \cdot 10^{-10}$	$8.70 \cdot 10^{-10}$
k [mD]	43.452	36.173
ϕ [–]	0.1642	0.1696
h [m]	41.223	35.180
f [–]	0.8030	0.6220
r_e [m]	4,254.42	9,150.17
r_D [–]	4.0180	8.0092

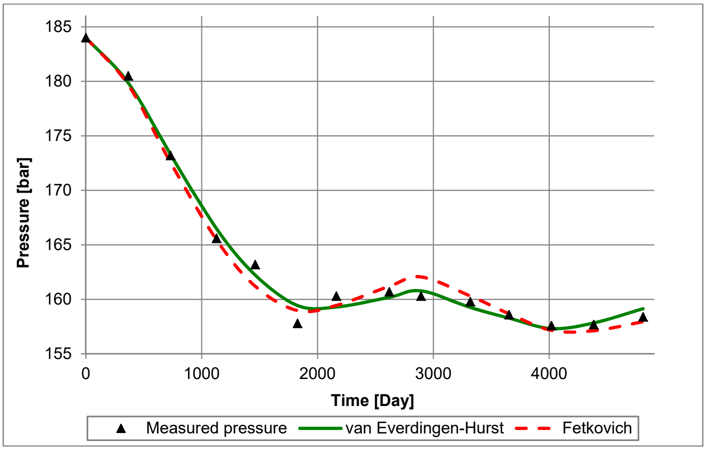

Fig. 11. Pressure as a function of time for the reservoir C

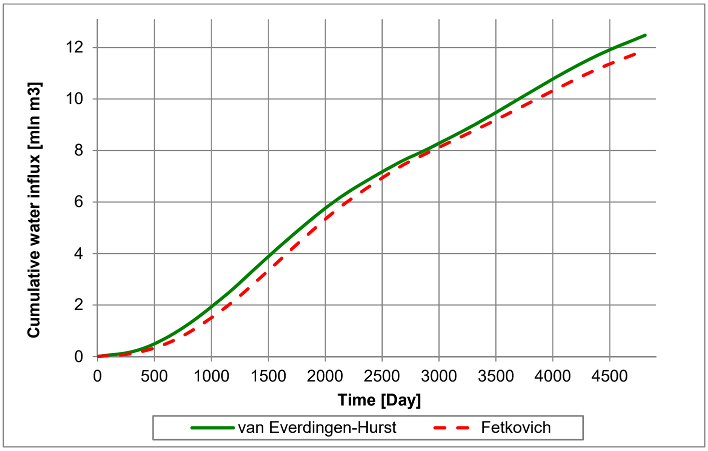

Fig. 12. Cumulative water influx as a function of time for the reservoir C

4.4. Analysis of reservoir D

The example of reservoir D presents the evaluation of compatibility between the determined values and the production data. The data covered a seven-year-long period of production and a five-year-long period of pressure buildup (Table D1). The model was calibrated based on the first seven years. The pressure buildup was evaluated based on the calibrated calculation model with the average reservoir temperature equal to 315 K.

TABLE 7

Estimated values and limits of the parameters – Reservoir D

Parameter	Input value	Min. value	Max. value
G_i [bln Nm^3]	2.2	1.8	2.5
C_w [1/Pa]	$5.80 \cdot 10^{-10}$	$2.90 \cdot 10^{-10}$	$8.70 \cdot 10^{-10}$
k [mD]	350	250	450
ϕ [–]	0.2	0.1	0.3
h [m]	50	40	60
f [–]	0.3	0.1	0.7
r_e [m]	2,000	1,000	10,000
r_D [–]	12	5	15

The parameters describing the aquifer are similar for both methods of calculating water influx. However, the petrophysical parameters of reservoir rocks are slightly different (Table 8). The determined pressures are in line with the measured pressures for both methods. This dependency can be seen clearly in the evaluation and the forecast (Fig. 13). The amount of the water influx is initially larger for the vEH method, while during the period of pressure buildup, the difference is reduced (Fig. 14). The coefficient of determination for both methods is close to one (Table D3). The aquifer can be considered active (Fig. D1). Points in the plot F/Eg vs. We/Eg are in accordance with the straight line with the slope equal to one (Fig. D2). It indicates the proper selection of the values of the parameters. A better compatibility was obtained for the vEH method.

TABLE 8

Determined values of the parameters – Reservoir D

Parameter	Output value	
	Fetkovich	van Everdingen Hurst
G_i [bln Nm^3]	2.134	2.041
C_w [1/Pa]	$5.65 \cdot 10^{-10}$	$3.23 \cdot 10^{-10}$
k [mD]	361.191	250.000
ϕ [–]	0.1838	0.1495
h [m]	40.000	58.643
f [–]	0.1343	0.1544
r_e [m]	2,112.74	2,016.21
r_D [–]	13.972	13.002

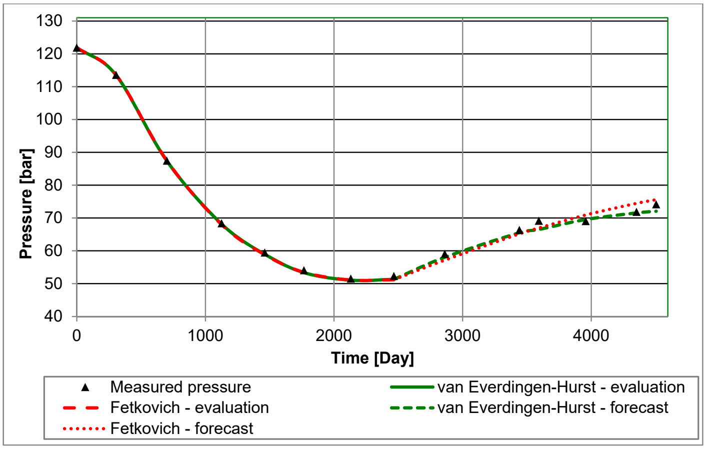

Fig. 13. Pressure as a function of time for the reservoir D

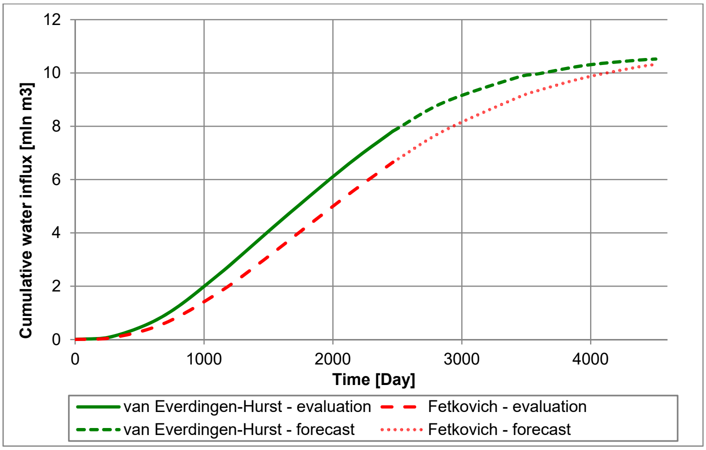

Fig. 14. Cumulative water influx as a function of time for the reservoir D

4.5. Analysis of reservoir E

The example of reservoir E presents the evaluation of compatibility between the determined values and the production data. The data covered a ten-year-long period of production and a three-year-long period of using the natural gas reservoir for a UGS (Table E1). The model was calibrated based on the data from the first ten years. The gas storage was evaluated, based on the calibrated calculation model. The forecast of three injection/withdrawal cycles of the high-methane natural gas was prepared. The average reservoir temperature was equal to 303 K.

The determined parameters for both methods are similar (Table 10). The determined and measured pressures are in line with one another. However, slight differences can be noticed in the forecast period (Fig. 15). The amount of water influx is compatible with both methods (Fig. 16). The coefficient of determination for the Fetkovich method is equal to 0.99930, while for the vEH

TABLE 9

Estimated values and limits of the parameters – Reservoir E

Parameter	Input value	Min. value	Max. value
G_i [bln Nm^3]	0.17	0.16	0.18
C_w [1/Pa]	$5.80 \cdot 10^{-10}$	$4.35 \cdot 10^{-10}$	$7.25 \cdot 10^{-10}$
k [mD]	35	30	40
ϕ [–]	0.17	0.15	0.20
h [m]	20	10	30
f [–]	0.5	0.1	1.0
r_e [m]	1,000	500	3,000
r_D [–]	10	5	15

method to 0.99931 (Table E3). The aquifer can be considered as moderate (Fig. E1). The points in the plot *F*/*Eg* vs. *We*/*Eg* are in accordance with the straight line with the slope equal to 0.98 (Fig. E2). It indicates the proper calibration of the mathematical model.

TABLE 10

Determined values of the parameters – Reservoir E

Parameter	Output value	
	Fetkovich	van Everdingen Hurst
G_i [bln Nm^3]	0.178	0.178
C_w [1/Pa]	$5.78 \cdot 10^{-10}$	$5.74 \cdot 10^{-10}$
k [mD]	37.745	33.762
ϕ [–]	0.1679	0.1686
h [m]	19.422	19.931
f [–]	0.6045	0.6588
r_e [m]	923.94	957.60
r_D [–]	5.457	5.004

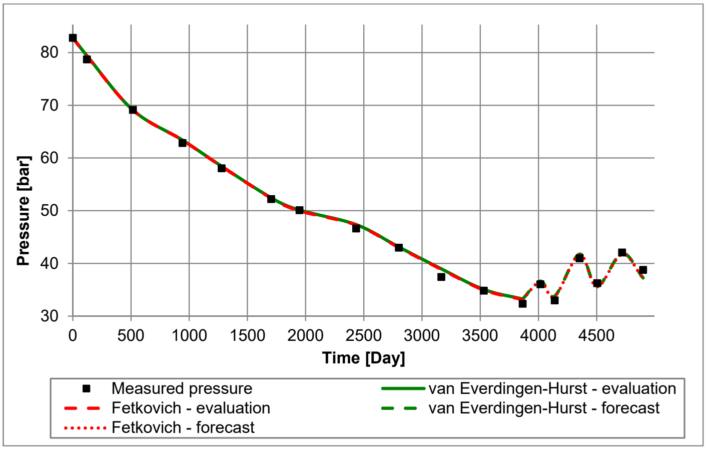

Fig. 15. Pressure as a function of time for the reservoir E

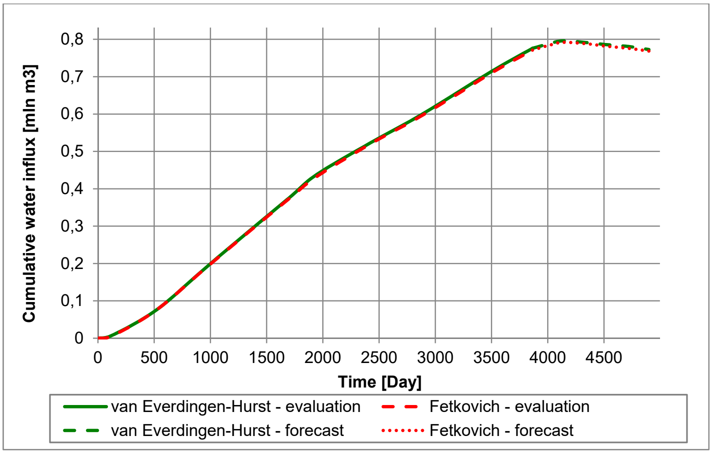

Fig. 16. Cumulative water influx as a function of time for the reservoir E

5. Comparison with commercial application

To validate the correct functioning of the application, a comparison with a commercial application was made. For that purpose, the MatBal 1.4 application released by Weatherford (EPS) Ltd. was used. The comparison includes not only model calibration but also production forecast. Notwithstanding high compatibility between the determined pressures resulting from the calibration of a model and the measured pressures, forecasting might be unsuitable. Therefore, the results from reservoir D and reservoir E were chosen and compared with the results from MatBal. In these examples, the forecasted values were compared with both the results from the MatBal application and the measured values. The same values and limits of the input parameters were used in the developed application and MatBal.

5.1. Comparison for reservoir D

To carry out the calibration of the mathematical model for reservoir D, the vEH method was used. The calibration based on historical data gives the results, which are almost equal for both MatBal and the developed application. The high compatibility was achieved in terms of pressures (Figs: 13, F1) and cumulative water influx (Figs: 14, F2). The buildup pressures obtained from the forecast differed from each other. The results from MatBal are significantly smaller than the measured ones and those calculated in the proposed application (Fig. 17).

5.2. Comparison for reservoir E

The Fetkovich method was used to carry out the calibration of the mathematical model for reservoir E. The calibration based on historical data gives the pressures, which are almost equal for both MatBal and the developed application (Figs:15, F3). Whereas the determined cumulative amount of water influx, which gradually increased during the period of production, was higher in MatBal. Subsequently, it remained stable during the period of working as UGS while slightly decreasing in the proposed application results (Figs: 16, F4). Pressures calculated in MatBal at the end of each injection process were significantly higher. This difference resulted in worse compatibility with the measured values (Fig. 18).

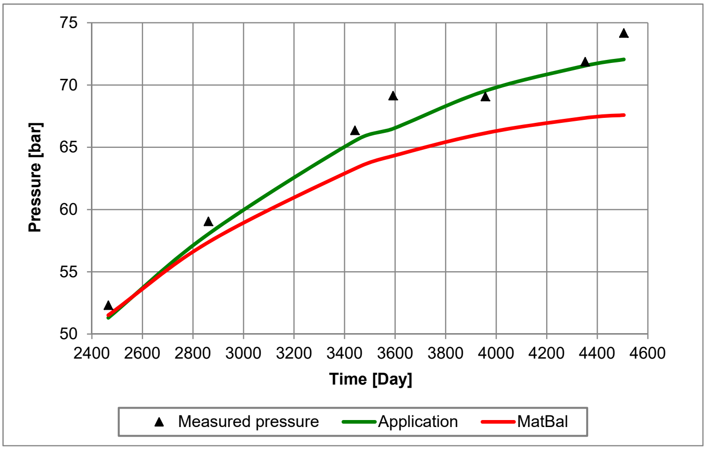

Fig. 17. Pressure as a function of time for reservoir D – comparison between measured pressures and the forecasted pressures obtained from the developed application and MatBal

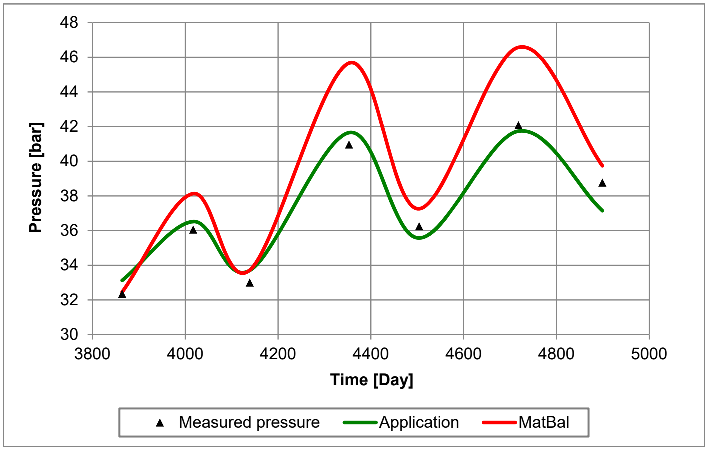

Fig. 18. Pressure as a function of time for the reservoir E – comparison between the measured pressures and the forecasted pressures obtained from the developed application and MatBal

6. Discussion

As a result of the optimisation process, very high compatibility between the determined pressures and the measured pressures was achieved. For every example, the calculated pressure values differ from the measured ones with a relative error of less than 2%. Almost every time, the obtained coefficients of determination for both methods were higher than 0.99 (Tables: A3, B3, C3, D3, E3, Figs: 7, 9, 11, 13, 15).

Proper calibration of the mathematical model is the most challenging for production data with fluctuations of the reservoir pressure. Such problems can be noticed in reservoir A (Fig. 11). This situation could be due to an irregular production, a lack of necessary measurements or a faulty data set. The most efficient approach is to provide the largest possible amount of data. The more information is provided, the more accurate the calibration model is.

The linear position of points in the HO plot and a suitable match between the determined and the measured pressures indicate the correct calibration of the mathematical model. It might be obtained for different input values of the parameters describing the reservoir and the aquifer. This can be observed for reservoir C (Table 6, Figs: 11, C2) and for reservoir D (Table 8, Figs: 13, D2). It relates to the optimisation algorithm, which searches for the best-fitted value until it finds the nearest local minimum. The minimum is represented by the output parameters and it might be different for the two methods. With ten output parameters, which influence the result, different values could probably result in the same solution.

One of the most crucial output parameters is the OGIP. The determined values of that parameter were presented in tables (Tables: 2, 4, 6, 8, 10) and HO diagnostic plots (Figs: A2, B2, C2, D2, E2). However, when comparing the values in the tables with these presented in the plots, some minor differences can be observed (Table 11). The intercept in the HO plot is evaluated using a linear regression method. The interpolated line has a slope close to one but not equal to it. As a result, the crossing point of the line and the Y axis is not the one determined in the optimization process.

TABLE 11

Differences in OGIP between the determined values and the values in HO plots for the Fetkovich method

Reservoir	**A**	**B**	**C**	**D**	**E**
Determined value [bln Nm^3]	5.200	0.195	5.967	2.134	0.178
Value in HO plot [bln Nm^3]	5.158	0.195	5.871	2.135	0.179

Notwithstanding the perfect match of the determined and the measured pressures in the presented example of reservoir D (Table: D3, Figs: 13, D2), a discrepancy in the amount of the influx water between the two methods of calculating water influx can be noticed. The foremost cause of that was the 4.5% difference in the OGIP (Table 8), which influenced the amount of gas that remains in the reservoir. This parameter differed up to 17% during the production process. With the compatibility of pressures, these differences compensate for one another.

In the example of reservoir E, the calculation model was calibrated based on the data from the production period. Furthermore, based on the calibrated model, the forecast of three injection/withdrawal cycles was made (Fig. 15). The best fit between the determined and the measured pressures was obtained for the first cycle. The following cycles have a slightly worse match. This result proves that the forecast is more reliable for shorter periods. Therefore, while forecasting long-term operations, considerable caution should be taken. To enhance the reliability, more measured points should be provided.

The comparison of the results from the developed application and those from MatBal demonstrates the importance of correct calibration. A well-calibrated model presents a more credible forecast, which could be a determining factor for a decision about further production.

In the example of reservoir E, the amount of water influx gradually decreased during the period of UGS (Fig. 16) while remaining stable in the MatBal results (Fig. F4). The movement of water in the reservoir during the injection/withdrawal process also affected pressure changes. Consequently, the pressures calculated in MatBal were overestimated. Whereas the results obtained in the proposed application were comparable to the measured ones. A reliable forecast could highly influence a decision about using this reservoir for the UGS purpose.

7. Conclusions

The assessment of the reservoir energy conditions, the gas reserves and the petrophysical parameters of a gas field is an essential part of credible further production forecasting.

The article presents the computer application, which was developed based on analytical methods and the Trust Region Reflective optimisation algorithm, which allows for the assessment of the production history of gas reservoirs in different energy conditions. With a set of historical data, the user can determine the parameters of a reservoir-aquifer system and use them to predict further gas field production.

The correctness of the calculations was validated using five case studies of the actual gas fields in the Polish Carpathian Foredeep. High compatibility between the computed and the real values of the reservoir pressure was obtained with a coefficient of determination equal to 0.99 and an average relative error of less than 2%. Furthermore, based on the cases of reservoirs D and E, the production forecast was created using the commercial MatBal application. The results of the reservoir pressures obtained from MatBal were overestimated by the measured values. The average relative error equated to 5%, while the same error obtained from the developed software was equal to 2%. The example of reservoir E presents using the application to forecast the injection/withdrawal cycles of a UGS. The results obtained from the application suggest that the pore volume available for the gas increased during the cycles, which is favourable in terms of using the reservoir as a UGS. Conversely, the results obtained from MatBal, which are burdened with a higher error, imply the stability of the amount of water influx into the reservoir and might lead to the wrong decision of using the reservoir as a UGS.

The proposed application is highly efficient and does not require building a complex numerical reservoir model. Together with other applications dedicated to solving specific problems, the proposed application could be used as an alternative to commercial reservoir simulators or as their supplementary software.

Author Contributions

Conceptualization, W.Ż. and J.B.; methodology, J.B., C.R.; software, W.Ż.; validation, W.Ż. and J.B.; formal analysis, J.B., W.Ż. and C.R.; investigation, J.B. and W.Ż.; writing – original draft preparation, W.Ż.; writing – review and editing, W.Ż., J.B. and C.R.; supervision, J.B. and C.R. All authors have read and agreed to the published version of the manuscript.

Funding

This research received no external funding.

Conflicts of Interests

The authors declare no conflict of interest.

References

[1] L.P. Dake, Fundamentals of Reservoir Engineering, Elsevier, Amsterdam (1978).

[2] P. Diamond, J. Ovens, Practical Aspects of Gas Material Balance: Theory and Application. SPE-142963. (2011). DOI: https://doi.org/10.2118/142963-MS

[3] J. Hagoort, Fundamentals of Gas Reservoir Engineering, Elsevier Science, New York (1988).

[4] D.A. Lupu, D.A. Stefanescu, I. Foidas, Analyzing and Forecasting the Performance of Water Drive Gas Reservoirs. AGH Drilling, Oil, Gas **36** (1), 143-159 (2019). DOI: http://dx.doi.org/10.7494/drill.2019.36.1.143

[5] L. Vega, R.A. Wattenbarger, New Approach for Simultaneous Determination of the and Aquifer Performance with No Prior Knowledge of Aquifer Properties and Geometry. SPE-59781-MS. (2000). DOI: https://doi.org/10.2118/59781-MS

[6] J.L. Pletcher, Improvements to Reservoir Material-Balance Methods. SPE-62882-MS. (2000). DOI: https://doi.org/10.2118/62882-MS

[7] F.W. Cole, Reservoir Engineering Manual. Gulf Publishing, Houston, TX (1969).

[8] B.C. Craft, M.F.Jr. Hawkins, Applied petroleum reservoir engineering, Second Edition, Prentice Hall Inc., Englewood Cliffs, NJ (1991).

[9] R.G. Agarwal, R. Al-Hussainy, H.J.Jr. Ramey, The importance of water influx in gas reservoirs. J. Petrol. Technol. **17** (11), 1336-1342 (1965). DOI: https://doi.org/10.2118/1244-PA

[10] J.A. Al-Ghanim, I.S. Nashawi, A. Malallah, Prediction of Water Influx of Edge – Water Drive Reservoirs Using Nonparametric Optimal Transformations. SPE 150662. (2012). DOI: https://doi.org/10.2118/150662-MS

[11] B. Wang, T.S. Teasdale, GASWAT-PC: A Microcomputer Program for Gas Material Balance With Water Influx. SPE-16484-MS. (1987). DOI: https://doi.org/10.2118/16484-MS

[12] J. Blicharski, Analytical modeling of the gas storage process in depleted natural gas reservoirs – selected aspects, The AGH University of Science and Technology Press, Krakow (2018).

[13] L.P. Dake, The Practice of Reservoir Engineering, revised ed.; Elsevier Science Publishers, Amsterdam (2001).

[14] T. Ahmed, P. McKinney, Advanced Reservoir Engineering, 1st ed., Gulf Professional Publishing (2005).

[15] M.J. Fetkovich, A simplified Approach to Water Influx Calculations-Finite Aquifer Systems. J. Petrol. Technol. **23** (07), 814-828 (1971). DOI: https://doi.org/10.2118/2603-PA

[16] A.F. Van Everdingen, W. Hurst, The application of the Laplace transformation to flow problems in reservoirs. J. Petrol. Technol. **1** (12), 305-324 (1949). DOI: https://doi.org/10.2118/949305-G

[17] I.S. Nashawi, A. Elkamel, Neural network model for the prediction of water aquifer dimensionless variables for edge-and bottom-water drive reservoirs. Energy and Fuel **13** (1), 88-98 (1999). DOI: https://doi.org/10.1021/ef980128q

[18] https://docs.scipy.org/doc/scipy/reference/generated/scipy.optimize.least_squares.html, accessed: 12.07.2020.

[19] http://www.applied-mathematics.net/LMvsTR/LMvsTR.pdf, accessed: 11.11.2019.

[20] http://www1.lsbu.ac.uk/water/physical_anomalies.html, accessed: 08.06.2020.

[21] A.Y. Dandekar, Petroleum Reservoir Rock and Fluid Properties, 2nd ed., CRC Press, Boca Raton, United States (2013). DOI: https://doi.org/10.1201/b15255

[22] http://www.fekete.com/SAN/WebHelp/FeketeHarmony/Harmony_WebHelp/Content/HTML_Files/Reference_Material/General_Concepts/Reservoir_Fluid_Properties.htm, accessed 18.11.2019.

[23] W.D. Jr. McCain, The Properties of Petroleum Fluids, 2nd ed.; PennWell Books, Tulsa, United States (1990).

[24] D. Havlena, A.S. Odeh, The Material Balance as an Equation of a Straight Line. J. Petrol. Technol. **15** (08), 896-900 (1963). DOI: https://doi.org/10.2118/559-PA

[25] D. Havlena, A.S. Odeh, The Material Balance as an Equation of a Straight Line. Part II – Field Cases. J. Petrol. Technol. **16** (07), 815-822 (1964). DOI: https://doi.org/10.2118/869-PA

[26] L. Clarke, R.J. Davies, J. van Hunen, S.E. Daniels, G. Yielding, Application of material balance methods to CO2 storage capacity estimation within selected depleted gas reservoirs. Petroleum Geoscience **23** (3), 339-352 (2017). DOI: https://doi.org/10.1144/petgeo2016-052

[27] A. Satter, G.M. Iqbal, J.L. Buchwalter, Practical Enhanced Reservoir Engineering: Assisted With Simulation Software. PennWell Books, Tulsa, (2008).

[28] C. Rybicki; J. Blicharski, Water movement problems in the process of gas production and underground gas storage. AGH Drilling, Oil, Gas **24** (1), 435-441 (2007).

APPENDIX A

TABLE A1

Gas field production data – Reservoir A

t, [day]	p, [bar]	G_p, [mln Nm^3]
0	152.4	0
731	135.9	587
1,461	124.3	1,118
2,192	110.3	1,630
2,922	101.2	2,037
3,653	89.7	2,478
4,749	72.1	3,134
5,479	57.7	3,588
6,210	47.7	3,933
8,401	28.4	4,598

TABLE A2

Gas compositions – Reservoir A

Composition	Mole percentage, [%]
methane – C_1	98.77
ethane – C_2	0.32
propane – C_3	0.14
isobutane – i-C_4	0.17
n-butane – C_{4+}	0.09
carbon dioxide – CO_2	0.01
nitrogen – N_2	0.50
hydrogen sulfide – H_2S	0.00
helium – He	0.00

TABLE A3

Statistical measures – Reservoir A

Statistical measure	Value	
	Fetkovich	van Everdingen Hurst
Coefficient of determination	0.99904	0.99900
Avg. absolute error [Pa]	80,055.4	77,859.3
Avg. relative error [%]	1.71	1.70
Max. absolute error [Pa]	321,700.2	335,792.9
Max. relative error [%]	11.33	11.83

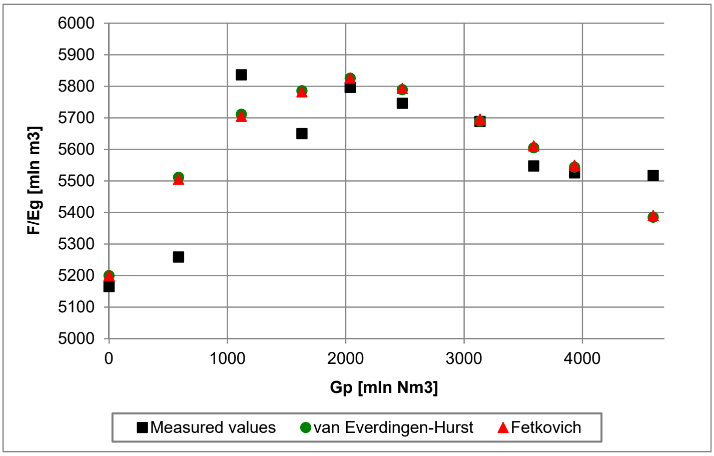

Fig. A1. Cole plot for the reservoir A

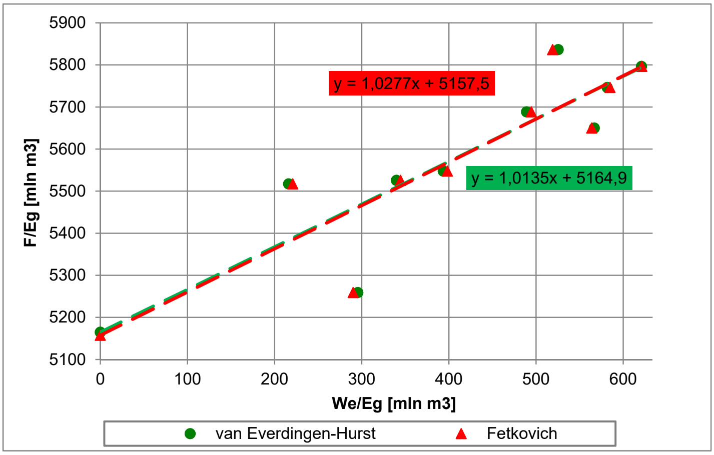

Fig. A2. Havlena-Odeh plot for the reservoir A

APPENDIX B

TABLE B1

Gas field production data – Reservoir B

t, [day]	p, [bar]	G_p, [mln Nm^3]	W_p, [m^3]
0	42.1	0	0
253	36.9	26.4277	3.211
606	30.3	62.0178	9.41
950	25.3	87.046	14.944
1,345	21	108.0509	18.934
1,706	19.8	120.2051	22.974
1,993	17.7	126.8203	30.504
2,464	17.3	131.1789	36.419
2,787	17	133.89	41.519
3,130	16.9	137.1142	44.619

TABLE B2

Gas compositions – Reservoir B

Composition	Mole percentage, [%]
methane – C_1	99.00
ethane – C_2	0.80
propane – C_3	0.20
isobutane – i-C_4	0.00
n-butane – C_{4+}	0.00
carbon dioxide – CO_2	0.00
nitrogen – N_2	0.00
hydrogen sulfide – H_2S	0.00
helium – He	0.00

TABLE B3

Statistical measures – Reservoir B

Statistical measure	Value	
	Fetkovich	van Everdingen Hurst
Coefficient of determination	0.99887	0.99886
Avg. absolute error [Pa]	21,940.9	22,299.3
Avg. relative error [%]	1.11	1.14
Max. absolute error [Pa]	69,047.1	71,015.3
Max. relative error [%]	3.49	3.59

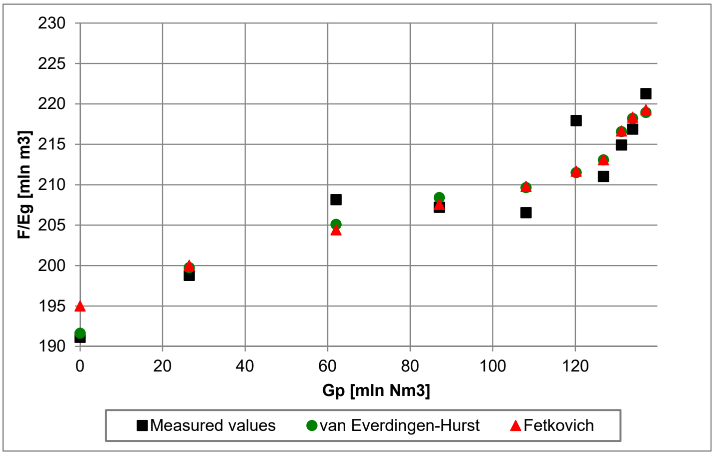

Fig. B1. Cole plot for the reservoir B

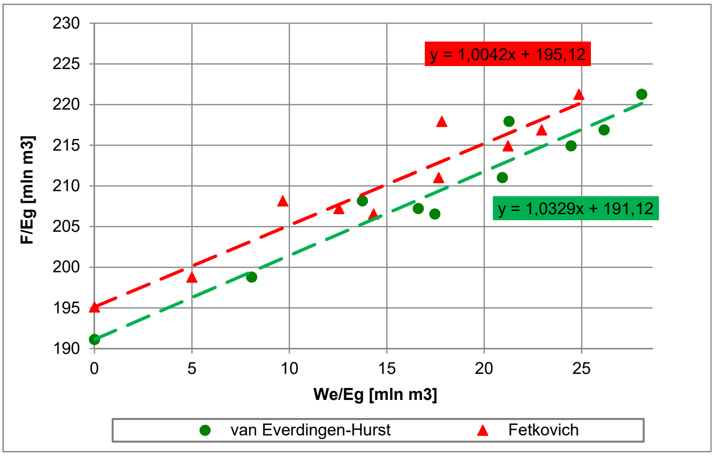

Fig. B2. Havlena-Odeh plot for the reservoir B

APPENDIX C

TABLE C1

Gas field production data – Reservoir C

t, [day]	*p*, [bar]	G_p, [mln Nm^3]
0	184.0	0.00
366	180.5	162.72
731	173.2	478.48
1,128	165.6	874.45
1,462	163.2	1,189.37
1,827	157.8	1,467.29
2,162	160.3	1,634.72
2,619	160.7	1,786.25
2,893	160.3	1,856.79
3,319	159.8	2,031.96
3,653	158.6	2,177.29
4,019	157.6	2,332.13
4,384	157.7	2,444.62
4,810	158.4	2,534.03

TABLE C2

Gas compositions – Reservoir C

Composition	Mole percentage, [%]
methane – C_1	73.32
ethane – C_2	1.01
propane – C_3	0.34
isobutane – i-C_4	0.07
n-butane – C_{4+}	0.37
carbon dioxide – CO_2	5.31
nitrogen – N_2	19.40
hydrogen sulfide – H_2S	0.09
helium – He	0.09

TABLE C3

Statistical measures – Reservoir C

Statistical measure	Value	
	Fetkovich	van Everdingen Hurst
Coefficient of determination	0.98839	0.99259
Avg. absolute error [Pa]	71,085.4	58,825.2
Avg. relative error [%]	0.437	0.363
Max. absolute error [Pa]	199,251.8	164,067.0
Max. relative error [%]	1.221	1.040

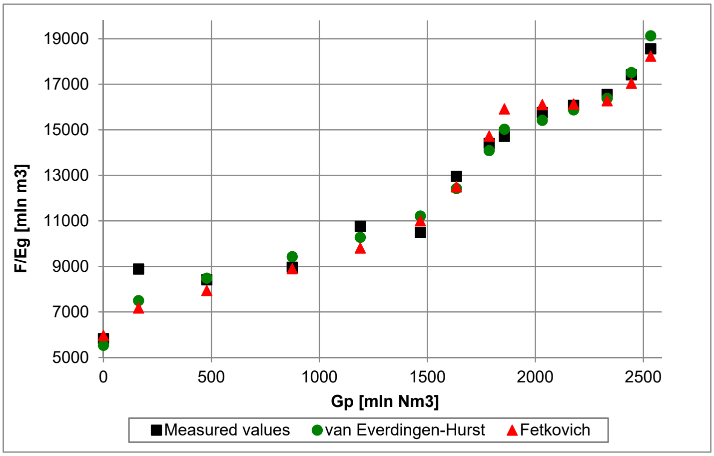

Fig. C1. Cole plot for the reservoir C

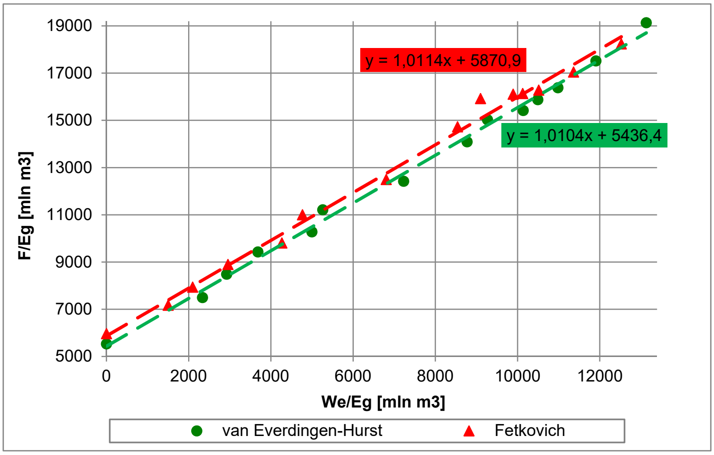

Fig. C2. Havlena-Odeh plot for the reservoir C

APPENDIX D

TABLE D1

Gas field production data – Reservoir D

t, [day]	*p*, [bar]	G_p, [mln Nm^3]
0	121.9	0.00
305	113.6	166.64
700	87.5	702.51
1,126	68.4	1,124.61
1,461	59.5	1,337.60
1,766	54.1	1,473.42
2,131	51.6	1,569.79
2,465	52.3	1,624.75
2,861	59.1	1,624.75
3,441	66.4	1,625.81
3,592	69.1	1,626.54
3,957	69.1	1,627.12
4,352	71.9	1,627.12
4,505	74.2	1,627.12

TABLE D2

Gas compositions – Reservoir D

Composition	Mole percentage, [%]
methane – C_1	96.90
ethane – C_2	1.10
propane – C_3	0.35
isobutane – i-C_4	0.06
n-butane – C_{4+}	0.19
carbon dioxide – CO_2	0.40
nitrogen – N_2	1.00
hydrogen sulfide – H_2S	0.00
helium – He	0.00

TABLE D3

Statistical measures – Reservoir D

Statistical measure	Value	
	Fetkovich	van Everdingen Hurst
Coefficient of determination	0.99997	0.99998
Avg. absolute error [Pa]	11,590.6	8,684.5
Avg. relative error [%]	0.198	0.153
Max. absolute error [Pa]	33,063.8	24,439.5
Max. relative error [%]	0.641	0.474

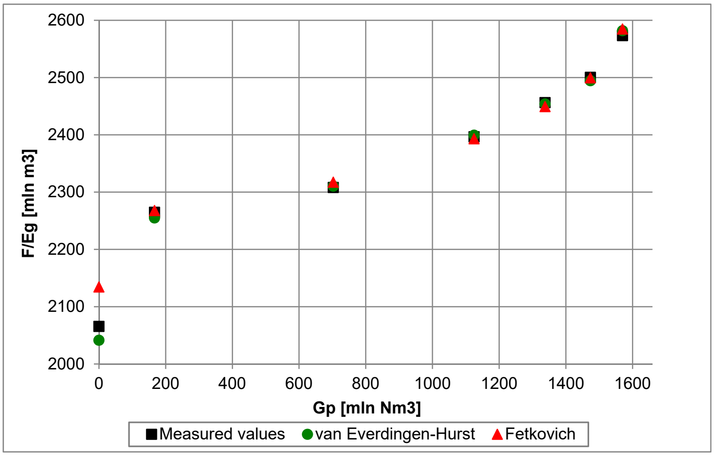

Fig. D1. Cole plot for the reservoir D

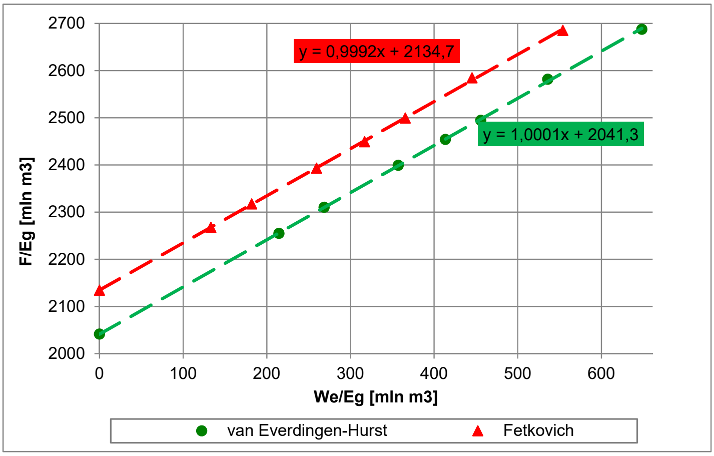

Fig. D2. Havlena-Odeh plot for the reservoir D

APPENDIX E

TABLE E1

Gas field production data – Reservoir E

t, [day]	p, [bar]	G_p, [mln Nm^3]	G_i, [mln Nm^3]	W_p, [m^3]
0	82.8	0.00	0.00	0.0
121	78.7	8.74	0.00	2.1
516	69.2	38.28	0.00	18.9
942	62.9	58.26	0.00	37.0
1,278	58.1	73.79	0.00	57.1
1,704	52.2	91.25	0.00	100.0
1,947	50.1	98.64	0.00	128.6
2,434	46.6	107.53	0.00	193.7
2,800	43.0	117.10	0.00	242.4
3,165	37.4	126.11	0.00	284.8
3,530	34.8	134.19	0.00	362.8
3,864	32.4	138.51	0.00	431.4
4,017	36.1	139.00	4.59	431.4
4,139	33.0	143.00	4.59	451.6
4,353	41.0	143.00	15.40	451.6
4,504	36.3	151.00	15.40	481.6
4,718	42.1	151.00	24.00	481.6
4,899	38.8	157.00	24.00	513.9

TABLE E2

Gas compositions – Reservoir E

Composition	Mole percentage, [%]
methane – C_1	97.00
ethane – C_2	1.20
propane – C_3	0.35
isobutane – i-C_4	0.06
n-butane – C_{4+}	0.08
carbon dioxide – CO_2	0.31
nitrogen – N_2	1.00
hydrogen sulfide – H_2S	0.00
helium – He	0.00

TABLE E3

Statistical measures – Reservoir E

Statistical measure	Value	
	Fetkovich	van Everdingen Hurst
Coefficient of determination	0.99930	0.99931
Avg. absolute error [Pa]	34,003.2	33,710.7
Avg. relative error [%]	0.727	0.718
Max. absolute error [Pa]	89,185.9	88,775.4
Max. relative error [%]	2.382	2.371

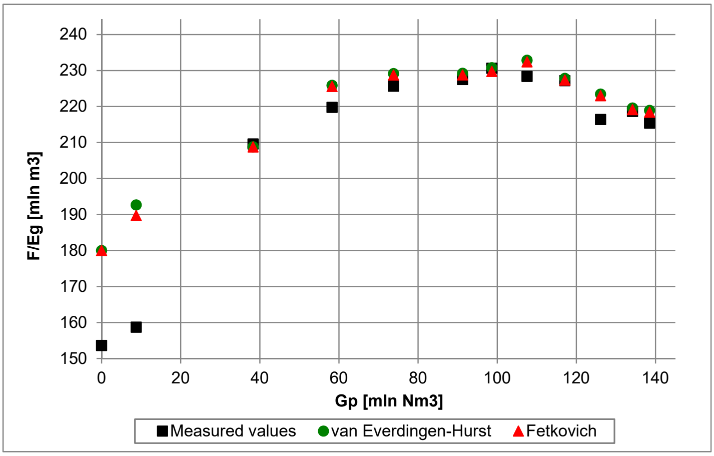

Fig. E1. Cole plot for the reservoir E

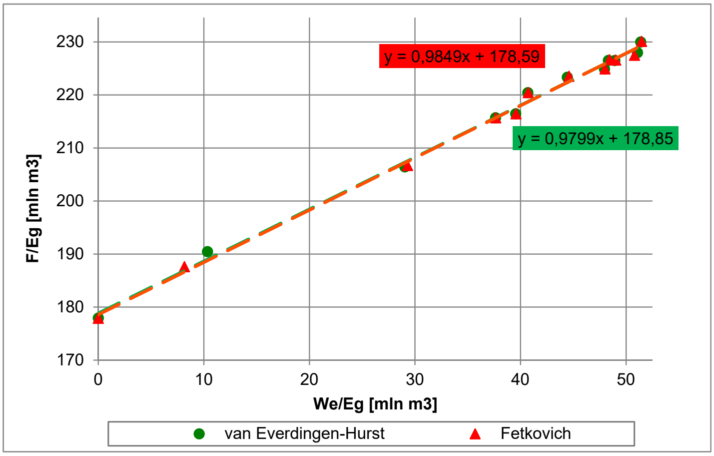

Fig. E2. Havlena-Odeh plot for the reservoir E

APPENDIX F

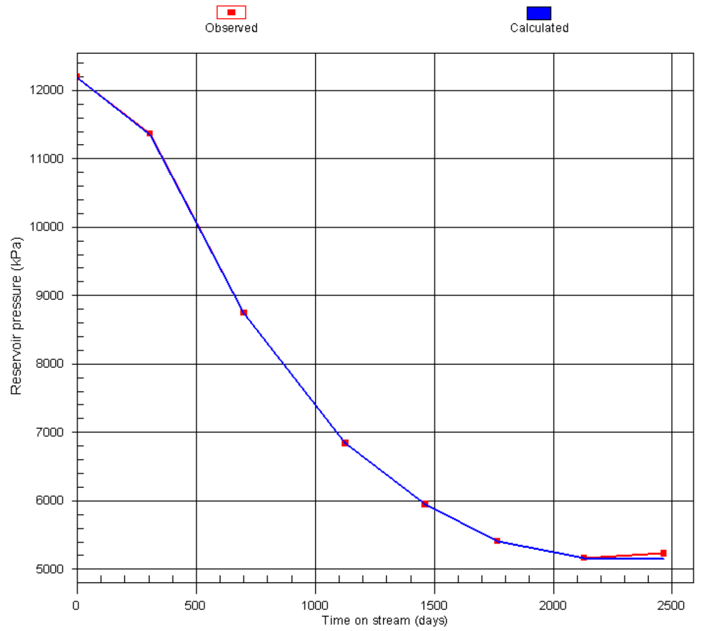

Fig. F1. Pressure as a function of time for the reservoir D – MatBal

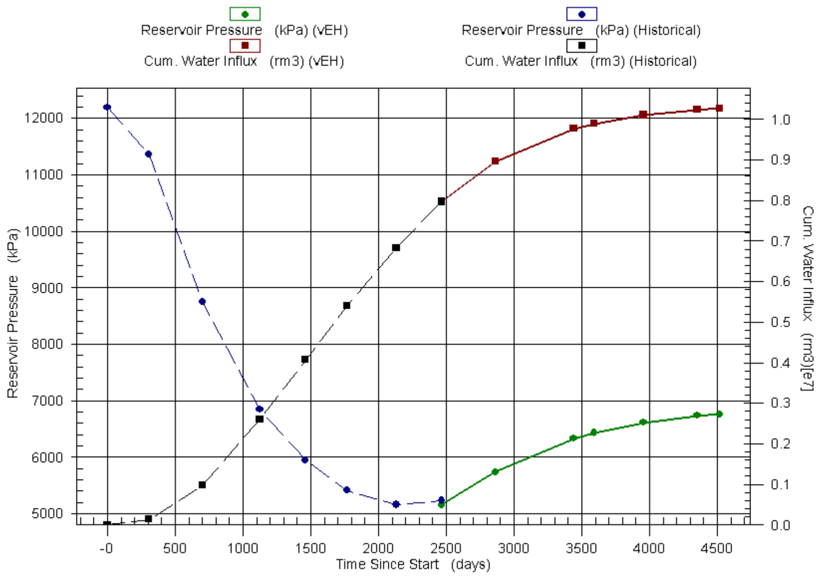

Fig. F2. Pressure and cumulative water influx as a function of time for reservoir D (forecast marked as a solid line)

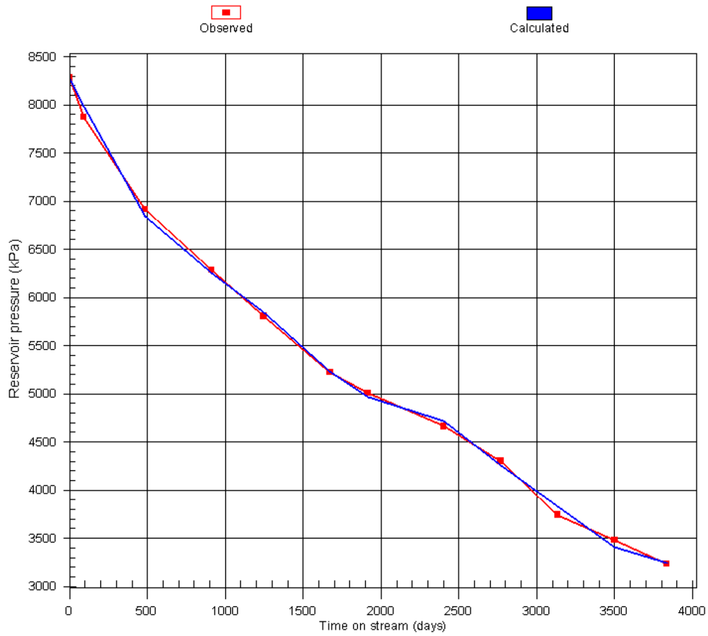

Fig. F3. Pressure as a function of time for reservoir E – MatBal

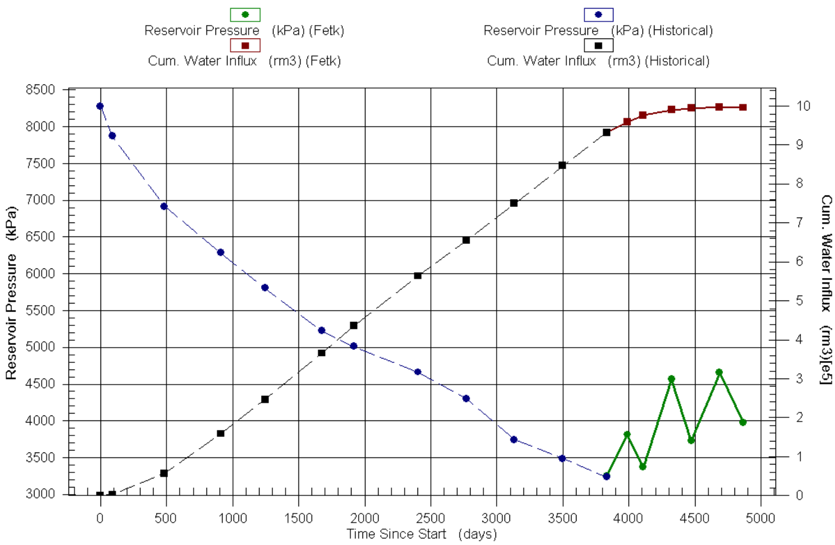

Fig. F4. Pressure and cumulative water influx as a function of time for reservoir E (forecast marked as a solid line)